

Revascularization and remodelling of pancreatic islets grafted under the kidney capsule

Sergio Morini,¹ Melissa L. Brown,² Luca Cicalese,² George Elias,² Simone Carotti,¹ Eugenio Gaudio^{1,3} and Cristiana Rastellini²

¹Department of Biomedical Research (CIR), University Campus Bio-Medico, Rome, Italy

²Department of Surgery, Division of Transplantation, University of Massachusetts, Worcester, MA, USA

³Department of Human Anatomy, University of Rome 'La Sapienza', Italy

Abstract

The revascularization and the structural changes resulting from interactions between the graft and the host were investigated in transplanted pancreatic islets under the kidney capsule. Islets were isolated from mice pancreata and transplanted in syngeneic diabetic animals. Graft-bearing kidneys were collected on different days post-transplant and processed for light microscopy, immunohistochemistry and transmission electron microscopy. A numerical analysis was performed in order to compare the percentage number of the different types of cells in native islets and at different time points after the transplant. Recipient animals reversed diabetes within 4 days. An intraperitoneal glucose tolerance test was performed to determine islet functionality under stressful conditions. During the initial few days post-transplant, the islets showed peculiar shapes and the graft tended to aggregate along the vessels. Starting at days 4–7 post-transplant, islets were revascularized from vessels connected to both the cortical and the capsular vascular network of the kidney. From day 7–14 post-transplant, the vessels progressively appeared more similar in features and size to those of *in situ* pancreatic islets. Both the percentage number of the different cell types and the distribution of Alpha, Beta and Delta cells inside the graft were significantly different as compared with intact islets, demonstrating quantitative and structural changes after the engraftment. No concomitant proliferation of Beta cells was detected using a bromodeoxyuridin staining method. Despite the fact that quick revascularization preserved a large mass of tissue, the remodelling process of the graft and the newly formed vascularization led to a different organization of the endocrine tissue as compared with intact *in situ* islets. This constitutes the morphological basis for alterations of the normal intercellular interactions and may explain the altered secretory cell function often observed in transplant.

Key words islets of Langerhans; revascularization; structure; transplantation; ultrastructure.

Introduction

Transplantation of isolated pancreatic islets is a promising approach for the treatment of type I diabetes (Tzakis et al. 1990; Pieper et al. 1995; Korbutt et al. 1997). Over the past decade this clinical approach has failed to produce satisfactory and consistent long-term results

(Bretzel et al. 1996; Rastellini et al. 1997; Hering & Ricordi, 1999). However, recent innovative strategies have been able to provide an increase in the success rate of insulin independence following pancreatic islet transplantation in diabetic patients (Shapiro et al. 2000; Ryan et al. 2005).

Even under the most successful protocols (Ryan et al. 2005; CITR, 2005, <http://spitfire.emmes.com/study/isl/>), islet mass seems to be a critical limitation to achieving insulin independence and within this limitation, interaction of multiple factors such as islet viability, functionality and engraftment are probably responsible for the outcome.

Correspondence

Eugenio Gaudio, MD, Department of Human Anatomy, University of Rome 'La Sapienza', Via Alfonso Borelli, 50, 00161 Rome, Italy. T: +39 06 4991 8050; F: +39 06 4991 8062; E: eugenio.gaudio@uniroma1.it

Accepted for publication 20 January 2007

The revascularization process of islet grafts is of major interest (Menger et al. 2001; Mattsson et al. 2006). In whole organ grafts, such as heart, kidney, intestine, liver or pancreas, the revascularization is supported by the pre-existing microvascular system of the organ, while isolated pancreatic islets are avascular grafts and necessitate the neo-formation of a microvascular network to re-establish nutritional blood supply. This condition leads to prolonged hypoxia as long as the islets are dependent on the diffusion of oxygen and nutrients from surrounding tissues. Therefore, from the isolation to the post-transplant period, pancreatic islets are in a prolonged vulnerable condition that could jeopardize cell survival (Davalli et al. 1996), as well as insulin secretion (Dionne et al. 1993), until they are revascularized by angiogenesis (Menger et al. 1989; Zhang et al. 2004).

Recent studies (El-Naggar et al. 1993; Wang et al. 1999; Morini et al. 2001, 2006) have demonstrated that islet isolation by collagenase, traumatic insult and prolonged hypoxia during the digestion and purification processes can cause changes of the normal structure in a substantial number of islets. These alterations have been considered the morphological basis for loss of regulated insulin secretion by isolated pancreatic islets (Pai et al. 1993). Besides the alterations following the isolation procedure, other structural changes could be expected as a consequence of the interaction between the transplanted islets and the host tissue (Davalli et al. 1996), especially regarding the microvascular organization.

The hypothesis leading our study was that the final structure of the engrafted islets could be quite different from that of *in situ* islets, thus affecting the fine secretory cell function and the final metabolic regulation. Therefore, the aim of this study was to investigate the process of revascularization and its relationship with the remodelling of the endocrine tissue transplanted under the kidney capsule. Although intrahepatic islet transplantation is commonly used in clinical protocols it does not appear to be the ideal location, especially in long-term follow-up. Because of the risks, including drug toxicity and lipotoxicity, alternative sites are under evaluation (Hering & Ricordi, 1999; Ricordi & Strom, 2004; Robertson, 2004; Shapiro et al. 2006). We chose the kidney as the site of transplant because it is an accurate model from a functional standpoint, and it allows us to investigate the vascularization of transplanted islets when these had engrafted enough to provide metabolic controls.

Materials and methods

Animals

In order to avoid alterations of the normal engraftment due to immunological components, we performed syngeneic islet transplantation on mice. C57BL/6 male mice (~12 weeks old) weighing ~30 g were used as pancreas (pancreatic islets) donors, islet recipients, and control for *in situ* islet study. Animals were purchased from Charles River Laboratory (New York, USA), housed in a standard animal facility and provided *ad libitum* with Purina rodent chow and tap water. All experiments were approved by the Institutional Animal Care and Use Committee and were performed following standard regulatory guidelines for research involving animals.

Pancreas procurement

Under Metofane (methoxyflurane, Pittman-Moore, Inc., Mundelein, IL, USA)-induced anaesthesia, a midline abdominal incision of the donor was performed. After cannulation of the pancreatic duct, cold (4 °C) collagenase (0.8 mg mL⁻¹; Sigma-Aldrich, St Louis, MO, USA) solution was injected. Following adequate distention, and quick exsanguinations through excision of the portal vein, the pancreas was harvested and stored on ice.

Islet isolation and purification

Islets were isolated by a modification of the semi-automated method described by Ricordi et al. (1992). Briefly, the harvested pancreata were loaded into a stainless steel digestion chamber and, under gentle agitation, were perfused with recirculating activated collagenase solution (flow rate 85 mL min⁻¹, temperature ~37 °C). Microscopic examination of dithizone-stained samples obtained serially at 2-min intervals (starting at the 6th minute of digestion) was used to monitor tissue digestion. With the appearance of dissociated intact islets, this process was ceased and the tissue was collected and washed (400 g for 3 min). Islets were further purified by centrifugation (800 g for 10 min) on discontinuous density gradients (1.108, 1.096, 1.037; Cellgro/Mediatech, Herndon, VA, USA). Washes after purification were performed at 800 g for 3 min and 400 g for 3 min.

Four isolations were performed for the entire study with 22 donors per isolation.

Islet assessment

Islets were assessed *in vitro* for number, purity and viability by dithizone and trypan blue dye exclusion (Sigma-Aldrich). Although trypan blue is poor and subjective for viability of multicellular aggregates, it is used (approved by FDA for pretransplant clinical islet assessment) in islet transplantation because it provides rapid viability information along with dithizone. Furthermore, islet functionality was determined by reversing chemically induced diabetes *in vivo*.

Diabetes induction and islet transplantation

Isolated islets were transplanted as fresh islets without being cultured. Recipient mice were rendered diabetic 4 days prior to islet transplantation by single streptozotocin injection (300 mg kg^{-1} i.v., tail vein; Sigma-Aldrich). Animals with blood glucose level (BGL) $> 300 \text{ mg dL}^{-1}$ for three consecutive days were included in the study. A total of 34 diabetic mice were transplanted. Under Metofane anaesthesia, approximately 600 islets per diabetic recipient were placed under the left kidney capsule (superior pole) following a left flank incision. Recipients of islet grafts who experienced reversal of diabetes within 1–4 days post-transplant were included in the study. Transplanted islets were considered to have engrafted when blood glucose levels of $< 200 \text{ mg dL}^{-1}$ were attained and maintained. BGL and body weight were monitored daily.

IPGTT

In normoglycaemic animals, at different post-transplant time points (4, 7, 14, 21 and over 50 days) islet graft functionality was assessed by intraperitoneal glucose tolerance tests (IPGTTs). Briefly, six animals for each time point were fasted overnight, and following the detection of baseline BGL, 2 g kg^{-1} body weight of glucose (in 0.5 mL of saline) was injected into the peritoneal cavity. BGL was then detected at 15, 30, 45, 60, 90 and 120 min after injection.

Study schedule

Graft-bearing kidneys were harvested and analysed on days 2, 4, 7, 14 and 21 post-transplant. Six animals were nephrectomized at each time point to perform histology, immunohistochemistry and transmission

electron microscopy (TEM). Four transplanted animals were used for the B-cell proliferation study.

Light microscopy

Graft-bearing kidneys were fixed in 4% buffered formaldehyde solution. While transplanted islets were easily visible on the surface, the kidneys were cut through transverse planes in order to obtain round slides containing some islets, about 1 mm thick. Specimens were then embedded in paraffin; 5- μm -thick sections were cut and stained with haematoxylin-eosin (HE) and routine techniques.

Immunohistochemistry

Samples of kidneys with transplanted islets, and pancreata of both normal and streptozotocin-treated animals were fixed in 4% buffered formaldehyde solution for 24 h at room temperature and embedded in paraffin of 57 °C melting point. Sections 5 μm thick were immunoperoxidase stained for glucagon, insulin and somatostatin.

The indirect immunohistochemical technique was used. After blocking the endogenous peroxidase activity, CAS Block (Zymed Laboratories, San Francisco, CA, USA) serum was applied to reduce non-specific background staining. For the localization of insulin-producing cells (B cells), we used as primary antibody the guinea-pig anti-insulin (Dako Corporation, Carpinteria, CA, USA) diluted 1 : 100, and the secondary antibody used was biotinylated rabbit anti-guinea-pig immunoglobulin (Zymed Laboratories) diluted 1 : 500.

To localize glucagon- and somatostatin-producing cells (A cells and D cells), we utilized as primary antibody rabbit anti-glucagon (Zymed Laboratories) diluted 1 : 50, and undiluted rabbit anti-somatostatin (Ymel, Rome, Italy), respectively. The secondary antibody used in both procedures was biotinylated goat anti-rabbit immunoglobulin (Zymed Laboratories).

For vascular detection we used as primary antibody goat polyclonal anti-von Willebrand factor (vWF) (Santa Cruz Biotechnologies, Inc., Santa Cruz, CA, USA) diluted 1 : 400. As secondary antibody we used LSAB Plus (Dako Corporation). We used rat anti-CD31 (BioLegend, San Diego, CA, USA) with biotinylated anti-rat IgG-B (Santa Cruz Biotechnologies, Inc.) as secondary antibody.

Sections were incubated overnight in the primary antibodies at 4 °C. After the application of the secondary

antibody the sections were incubated with streptavidin-peroxidase complex (Zymed Laboratories), and the subsequent development was performed with diaminobenzidine to yield a brown colour reaction. Sections were counterstained with Mayer's haematoxylin to facilitate nuclear identification. Controls were performed to exclude non-specific staining.

5-Bromo2'-deoxy-uridine (BrdU) staining

Beta cell proliferation was detected by BrdU incorporation. At day 7 and at day 14 post-transplant two animals were injected with BrdU (10 mL kg⁻¹). Three total injections were performed 24 h apart and the animals were killed 6 h following the last injection. Graft-bearing kidneys were prepared in paraffin-embedded sections and stained following the manufacturer's directions (ROCHE Applied Sciences, Indianapolis, IN, USA) and evaluated by immunofluorescence. Negative and positive controls were included. As positive control we used pregnant mice, in which islet hyperplasia due to B-cell replication is known to occur.

Transmission electron microscopy (TEM)

To obtain better fixation of the endothelial cells, kidneys for TEM observations were perfused through the descending aorta with buffered glutaraldehyde solution for 5 min before being harvested from the animals. Kidneys were then immersed in 2.5% phosphate-buffered (0.1 M, pH 7.4) glutaraldehyde solution for 48 h at 4 °C. Specimens, about 1 mm square, and containing transplanted islets, were cut from the surface of the kidney, washed in 0.1 M phosphate buffer and post-fixed in 1% OsO₄ for 2 h at 4 °C. Samples were then dehydrated through a graded ethanol series and propylene oxide and embedded in Epon 812 for 48 h. Semithin sections (0.5–1 µm thick) were cut with a glass knife on a Top Ultra 170 ultramicrotome (Pabish, Milan, Italy) and stained with methylene blue to select representative areas. Ultrathin sections were cut with a diamond knife, stained with uranyl acetate and lead citrate and observed via a Zeiss EM9A (Carl Zeiss, Oberkochen, Germany) transmission electron microscopy.

Numerical analysis

We considered the following for numerical analysis: up to 200 islets randomly chosen from six normal

pancreata; a similar amount of transplanted islets, taken from the pellet obtained after each isolation; all the samples with transplanted islets for each time point. Serial sections were stained with immunoperoxidase for glucagon, insulin and somatostatin. The percentage number of the different types of cells was calculated by counting A, B and D cells present in each islet. Comparisons between the percentage number of cells in *in situ* islets and in transplanted islets at different time points were statistically evaluated by Student's *t*-test for unpaired values.

Results

Pancreatic islet isolations were successfully performed. Comparable numbers of islets, value for IEq, purity and viability were obtained from the four isolations, as detailed in Table 1. Transplanted animals in this study reversed diabetes (BGL < 200 mg dL⁻¹) within 2 days post-transplant. Nephrectomies performed at the various time points resulted in the recurrence of diabetes in the following 24–48 h (Fig. 1a).

When transplanted islets were stimulated by glucose injection an abnormal response was observed in the immediate post-transplant period (2 and 4 days) (Fig. 1b, Table 2). Improved functionality in response to glucose challenge was observed over follow-up time.

Day 2

In the 2 days following transplantation under the kidney capsule, the graft appeared as an isolated mass

Table 1 Assessment of isolated mouse pancreatic islets

Isolation no.	Islet no.*	IEq†	Purity (%)‡	Viability (%)§	Function¶
1	3800	4780	85	89	8/8
2	4600	5400	75	92	9/9
3	4750	5480	80	96	9/9
4	3990	4810	85	95	8/8

*Number of islets counted on dithizone-stained fresh samples.

†Number of islets counted on dithizone-stained fresh samples with regard to diameter (50–100, 100–150, 150–200, 200–250 µm) and averaged to a diameter of 150 µm.

‡Dithizone-stained vs. unstained tissue.

§By trypan blue dye exclusion.

¶*In vivo* reversibility of chemically induced diabetes (in mice) by transplantation of ~600 IEq, under the kidney capsule.

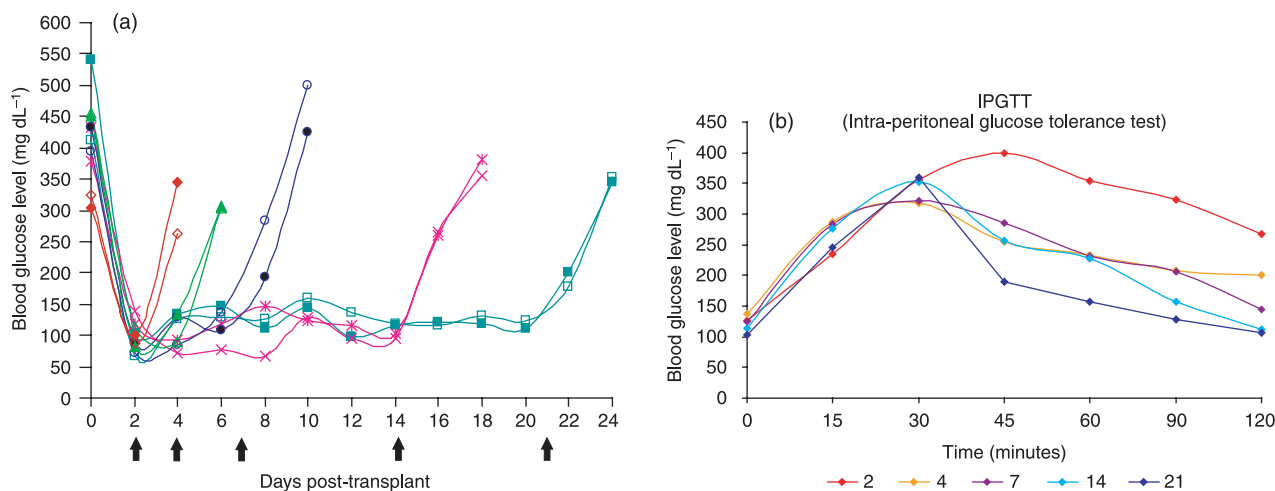


Fig. 1 *In vivo* functionality of transplanted pancreatic islets. (a) Blood glucose level determined before the injection of streptozotocin (STZ), just before the transplant (day 0) and in the post-transplant follow-up. Note the induction of diabetes, the stable normalization of glycaemia approximately 3 days after the transplant, and the re-induction of diabetes after the nephrectomy (†). (b) Intraperitoneal glucose tolerance tests (IPGTTs) performed on six animals for each time point (see also Table 2). After the intraperitoneal injection of glucose, blood glucose levels were measured at 15, 30, 45, 60, 90 and 120 min. An abnormal response was observed in the immediate post-transplant period (2 and 4 days). Animals at 21 days after the transplant showed the best response with lower levels of glycaemia at 45 min post-glucose infusion and normal levels after 120 min, while at 7 and 14 days an intermediate response to the test was observed.

Table 2 Results of the IPGTTs for each time point post-transplant

	Time 0	15 min	30 min	45 min	60 min	90 min	120 min
Day 2 post Tx	126.2 ± 19.9	234.5 ± 31.9	356.0 ± 64.6	399.5 ± 34.5	354.7 ± 35.9	323.7 ± 44.7	267.0 ± 17.3
Day 4 post Tx	138.0 ± 50.6	287.1 ± 52.5	318.0 ± 18.5	255.2 ± 30.2	232.5 ± 26.7	208.2 ± 28.7	199.7 ± 45.3
Day 7 post Tx	124.2 ± 16.7	283.0 ± 29.1	322.1 ± 33.2	285.5 ± 48.2	231.0 ± 30.1	206.5 ± 35.4	145.2 ± 28.8
Day 14 post Tx	113.5 ± 12.8	276.2 ± 26.3	352.7 ± 32.9	257.5 ± 43.5	227.2 ± 43.6	158.0 ± 39.7†	112.3 ± 14.1*
Day 21 post Tx	102.5 ± 26.9	245.2 ± 35.2	358.7 ± 49.1	190.5 ± 38.2‡	157.2 ± 22.9‡	128.7 ± 12.7*	106.0 ± 23.2*

† $P < 0.05$ vs. day 2, 4 and 7 post-transplant.

* $P < 0.01$ vs. day 2, 4 and 7 post-transplant.

‡ $P < 0.01$ vs. day 2, 4, 7 and 14 post-transplant.

of islets and fragments of endocrine tissue dispersed into a largely oedematous and sometimes haemorrhagic connective tissue. Degenerated exocrine tissue, mostly consisting of small ducts, lymphatic and soft tissue elements, was often present (Fig. 2).

The islets appeared in round or oval shapes sometimes showing irregular outlines lacking the capsule. The inner part of the largest islets appeared as an indistinct mass of necrotic tissue surrounded by apparently preserved cells (Fig. 2). Signs of necrosis were generally not evident in smaller or fragmented islets.

B cells appeared pale under immunoperoxidase staining for insulin; occasionally, many small granules were dispersed into the connective tissue. A and D cells

formed an incomplete layer around the B-cell core and appear normally stained.

Day 4

Oedema of the soft tissue was already present. The necrotic zones inside and outside the islets were often infiltrated by white blood cells and fibroblasts, and initial fibrosis and signs of vascular proliferation were observed into the necrotic core of some islets. The residual islets tended to fuse, forming clusters of endocrine tissue.

The peripheral cells at the surface of the islets, or of the islet fragments, tended to arrange along the vessels,

and initial angiogenesis and vascular proliferation were detectable (Fig. 3).

As a consequence of the necrosis in the core, the distribution of peripheral cells along the vessels, and the reaggregation of the residual endocrine tissue, the islets assumed odd shapes not seen in native islets (Fig. 4).

Immunohistochemistry revealed that the peripheral crown of A and D cells was largely incomplete and irregular in thickness. In contrast to intact islets, many B cells were usually present in the most peripheral layer of the islets.

Day 7

Oedema and vessel congestion were markedly reduced and the soft tissue appeared quite normal. The endocrine tissue formed large clusters of islets included between the renal parenchyma and the fibrous capsule. Thin fibrous septa accompanied by small vessels divided the parenchyma of the re-aggregated endocrine tissue, and collagen fibres tended to form a new thin connective capsule. Fibroblasts scattered around the islets were actively synthesizing matrix components and collagen fibres (Fig. 5).

Blood vessels of the host were located at the periphery of the endocrine parenchyma. Arising from these vessels, many new small vessels were growing, progressively penetrating into the islets (Fig. 6), and showing positive vWF immunostaining. TEM observation confirmed the presence of endothelial cells, lacking a basal lamina, proliferating inside the islet parenchyma. They formed sprouts typical of angiogenesis without defining a capillary lumen (Fig. 7). In addition to capillary sprouts, a variable number of vessels, able to support blood flow, were located within the peripheral cells and into the core of the islets. Endothelial cells presented a variable mass of cytoplasm, showing irregular thickness, large nuclei, mitochondria and packed rough endoplasmic reticulum (Fig. 8). The capillary wall often showed an extremely attenuated thickness, with a basal lamina supported by sparse collagen fibres. The thinnest portions of the plasmatic membrane presented fenestrations or pores where the endothelial cell interfaced with endocrine cells (Fig. 9). Scattered along the outside of capillaries were some pericytes and fibroblasts.

Immunoperoxidase staining for glucagon and somatostatin showed a distribution of cells often different from that of intact islets because A and D cells were

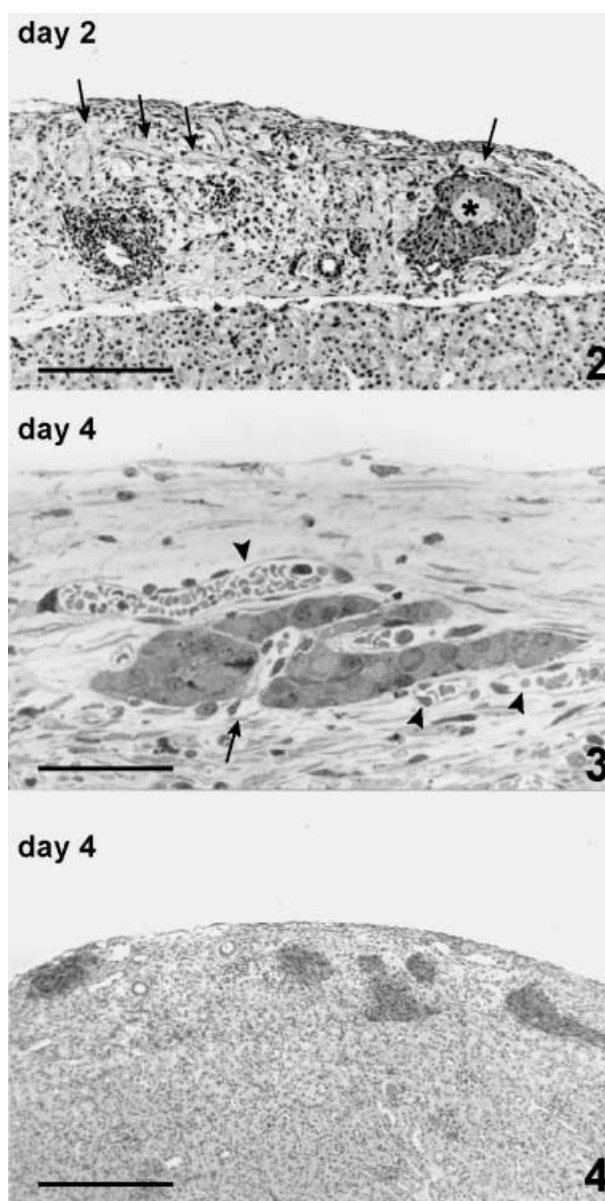


Fig. 2 Graft at day 2 post-transplant. A large, marginally located islet shows a necrotic core (*). Soft tissue appears largely oedematous, with infiltration of blood cells and congestion of blood (arrow) and lymphatic vessels. Fragments of islets and residual exocrine tissue are also present. Haematoxylin and eosin stain, 125 \times , scale bar = 200 μ m.

Fig. 3 Fragment of islet at day 4 post-transplant. These cells are disposed in a single or double layer close to pre-existing blood vessels (arrowhead) from which vascular proliferation is also visible (arrow). Semithin section, methylene blue stain, 400 \times , scale bar = 50 μ m.

Fig. 4 Graft at day 4 post-transplant. Transplanted islets showing irregular shape tend to aggregate forming clusters. Necrotic zones inside the connective tissue of the kidney capsule are almost completely repaired by macrophagic cells and proliferating fibroblasts. Some residual exocrine ducts are also present. Immunoperoxidase stain for insulin, 80 \times , scale bar = 260 μ m.

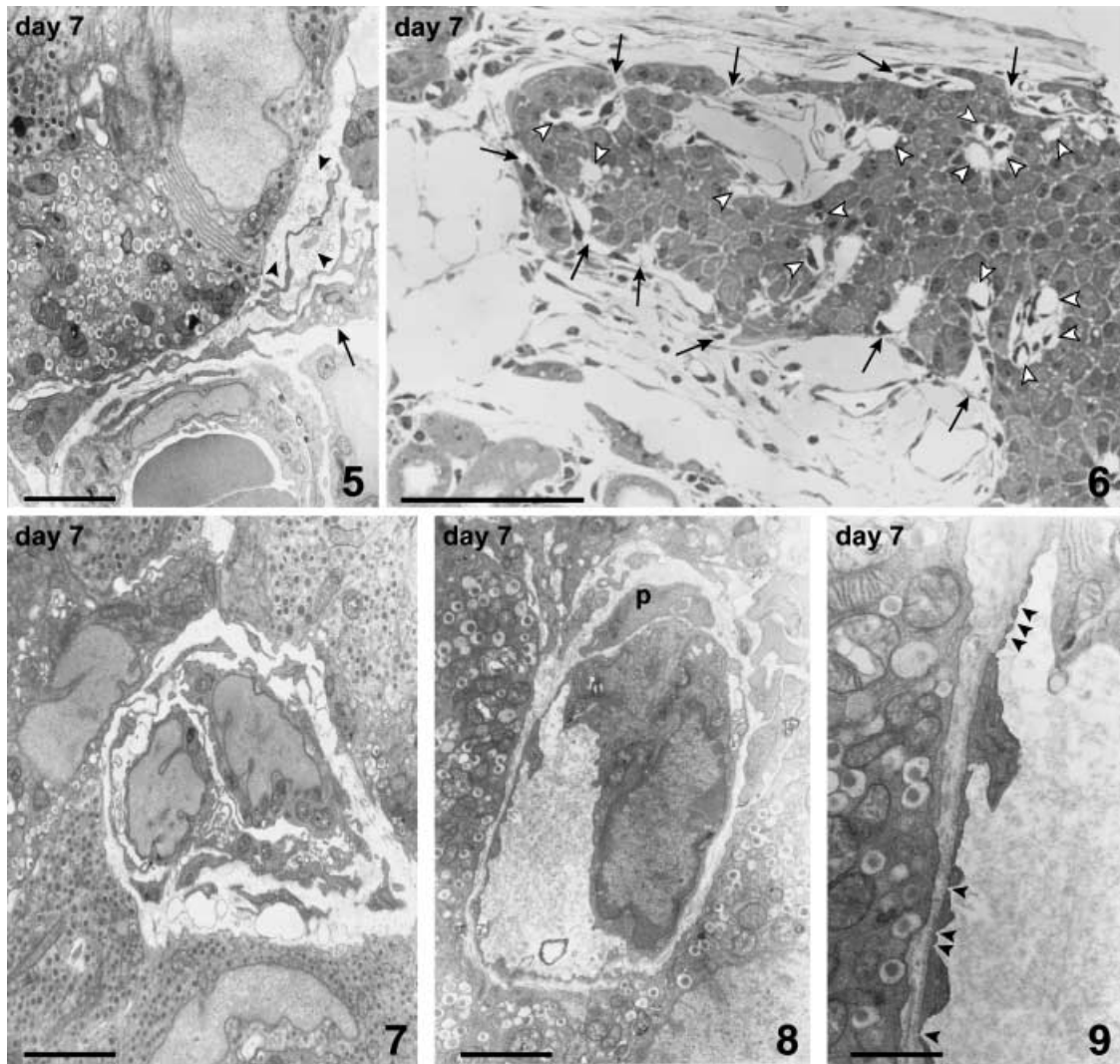


Fig. 5 Periphery of an islet at day 7 post-transplant. Long and slender processes of fibroblasts (arrow) secreting collagen fibrils (arrowheads) surround the islet and a vessel of the kidney capsule. TEM, scale bar = 2.5 μm .

Fig. 6 Islet at day 7 post-transplant. Arising from the vessels running along the outer surface of this large islet, many new vessels (arrows) are growing and penetrating from all directions towards the inner part of the endocrine parenchyma. Some vessels, lined by endothelial cells, are also visible in the islet parenchyma (arrowheads). Semithin section, methylene blue stain, 200 \times , scale bar = 100 μm .

Fig. 7 Angiogenesis at day 7 post-transplant. Two proliferating endothelial cells assume a sprout feature penetrating between B cells. They do not present a basal lamina and their processes are encircling a lumen that appears as a thin cleft between the two cells. TEM, scale bar = 3 μm .

Fig. 8 Capillary from the core of an islet at day 7 post-transplant. This capillary is lined by a single endothelial cell containing cytoplasm. A basal lamina surrounds the capillary; a perivascular cell (p) is also visible. TEM, scale bar = 2.5 μm .

Fig. 9 Detail of fenestrations (arrowheads) closed by a very thin diaphragm in the thinner part of the capillary wall. TEM, scale bar = 1 μm .

present inside the islet mass, often surrounded by B cells (Fig. 10).

Days 13–14

Signs of the remodelling process were no longer present at this time point. Peculiar structures formed

by endocrine cells distributed around capillary vessels were easily recognized, and these resembled the cell cords that constitute the morpho-functional unit inside the pancreatic islet (Fig. 11). The vessels located inside the islets showed positive vWF immunostaining, and poorer staining performances with CD31. Angiogenesis was rarely detectable via TEM observation, and a

Table 3 Percentage number of the various endocrine cell types present in transplanted islets (Tx) at different time points compared with *in situ* intact islets

	<i>In situ</i>	Isolated islets	day 2 post Tx	day 4 post Tx	day 7 post Tx	day 14 post Tx	day 21 post Tx
A cells	24.45 ± 3.12*	9.85 ± 4.63**	10.92 ± 6.32**	15.14 ± 7.91	13.02 ± 5.58	13.57 ± 6.97	13.81 ± 3.94
B cells	71.08 ± 3.06*	87.03 ± 7.24**	86.16 ± 6.41**	81.60 ± 8.22	84.39 ± 5.80	83.35 ± 7.38	83.84 ± 3.63
D cells	4.46 ± 1.37†	3.12 ± 1.38	2.92 ± 1.17	3.26 ± 1.32	2.58 ± 1.28	3.08 ± 1.41	2.35 ± 1.15

* $P < 0.001$ vs. isolated and transplanted islets.

† $P < 0.01$ vs. isolated and transplanted islets.

** $P < 0.01$ vs. transplanted islets at day 4.

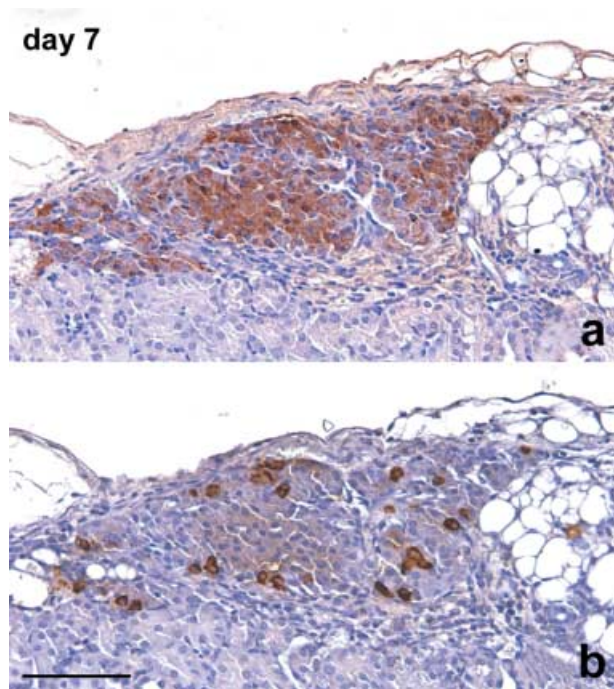


Fig. 10 Consecutive sections of islets re-aggregated in a cluster. A large number of cells show positive staining for insulin (a). Also, the peripheral layer of the cluster is largely represented by B cells. Some glucagon-stained A cells are singly scattered peripherally and also in the inner part of the cluster (b). Immunoperoxidase stain for (a) insulin, (b) glucagon, 200 \times , scale bar = 150 μ m.

variable number of capillaries were clearly visible inside the graft. Endothelial cells generally encircled a well-defined lumen with fenestrations towards the adjacent endocrine cells. The inner capillaries originated from the vessels running around the periphery of the islet. The outer vessels were connected to both the capsule and the cortical vascular network of the kidney (Fig. 11), so that the resulting blood flow of a single engrafted cluster of islets was supplied by different microvascular districts.

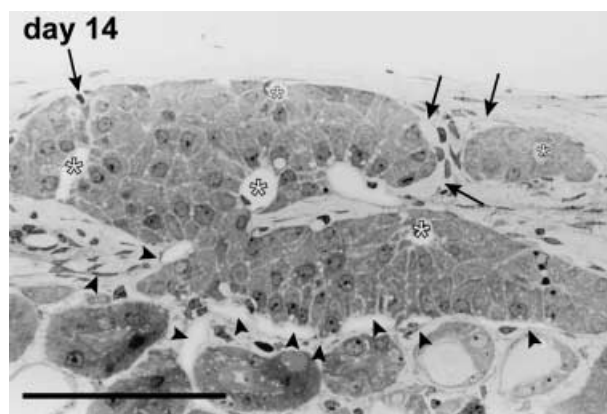


Fig. 11 Microvascular network of an islet at day 14 post-transplant. The endocrine cells form cordal-like structures disposed radially around capillaries (*) located inside the islet parenchyma, in most of the cases completely surrounded by endocrine cells. The vessels supplying this islet arise from host vessels located at the periphery of the islet. They are connected to the microvascular network of both the renal parenchyma (arrowheads) and the capsular district (arrows). Semithin section, methylene blue stain, 400 \times , scale bar = 100 μ m.

Immunohistochemistry did not show differences in the percentage number and the distribution of the different cell types with respect to the previous time points (Table 3).

Day 21

No substantial changes were observed as compared with days 13–14.

In situ islets

In situ islets were round or oval, had variable dimensions and consistently exhibited a very thin connective capsule that divided endocrine cells from exocrine tissue. A and D cells were scattered in the periphery of

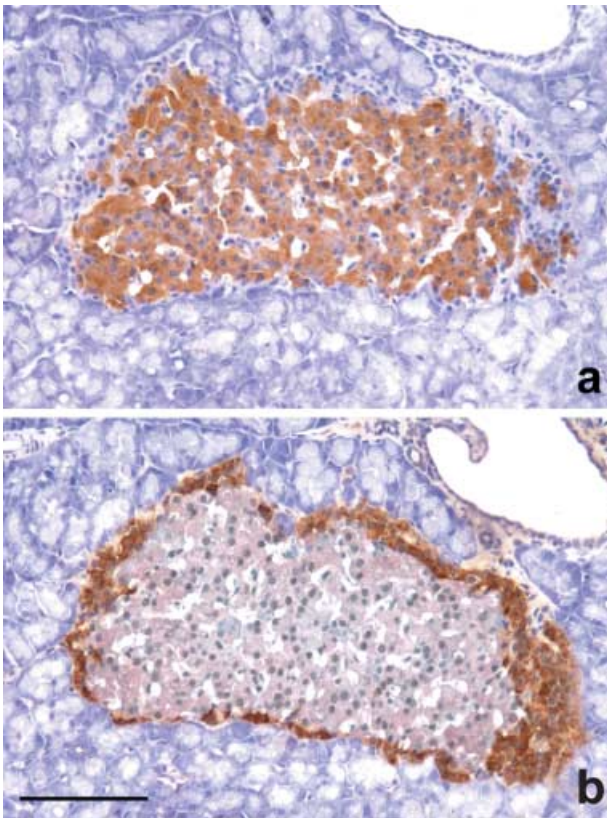


Fig. 12 Consecutive sections of *in situ* islets. In (a) the insulin-stained B cells occupy the core of the islet. They are surrounded by a nearly complete crown of unstained cells that are positive for glucagon, as shown in (b). Immunoperoxidase stain for (a) insulin, (b) glucagon, 200 \times , scale bar = 200 μ m.

the islet, and the largest islets showed a complete crown-like layer of 2–3 stratified cells, while the core of the islets contained only B cells (Fig. 12).

BrdU staining

Beta cell proliferation was not detected within engrafted pancreatic islets (Fig. 13). Proliferating beta cells could only be detected during the last third of pregnancy in both *in situ* pancreatic islets and transplanted islets, as expected (positive control).

Numerical analysis

The percentage number of the different cell types of *in situ* islets and at different time points following transplantation is given in Table 3. The percentage number of A, B and D cells in both isolated and transplanted islets was significantly different from that of

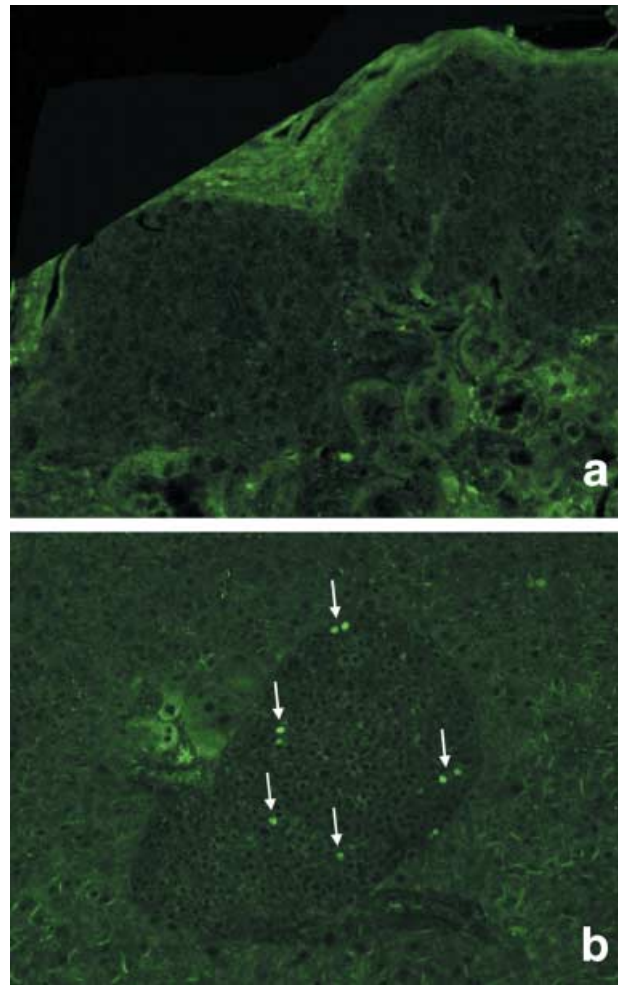


Fig. 13 BrdU incorporation for detection of proliferating islet cells. No evidence of proliferating cells within islets transplanted under the kidney capsule is detected (a). For comparison, proliferation (arrows) is clearly observed in native pancreatic islets of pregnant mice as positive control (b).

in situ islets. In particular, owing to the isolation process, a large percentage of the most peripheral cells (A and D) was lost, while the highest percentage of B cells was preserved. This condition persisted with slight changes up to day 2 post-transplant. At day 4, the percentage of B cells decreased, probably as a consequence of central necrosis, and the percentage of A cells increased significantly. No significant differences in the percentage of the different types of cells were found in the following periods.

Discussion

As we have previously shown (Morini et al. 2006), isolated pancreatic islets undergo structural and ultrastructural

changes, with complete loss of the microvascular network. The latter condition made the early period following transplantation critical for cell survival, until the islets became vascularized by a newly formed microvascular network arising from host vessels within 10–14 days (Vajkoczy et al. 1995; Menger et al. 2001). However, the present study has shown that many different phenomena occur before the engraftment becomes stable.

During the initial phase following transplantation some islets tended to fuse forming quite large clumps (Davalli et al. 1996), with 'contact' between the most peripheral cells and pre-existing vessels of the host. These vessels appeared largely dilated and congested, suggesting the presence of a possible inflammatory condition, probably consequent to both the surgical manipulation to introduce the islets under the kidney capsule and the presence of exocrine tissue, which is known to be less resistant to hypoxia, trauma and nutritional deficiency (Heuser et al. 2000; Barshes et al. 2005).

As a consequence of the new situation, most peripheral cells were able to survive because of their proximity to vessels that allowed an adequate blood supply. However, necrosis observed in the core of the largest islets was certainly due to hypoxia (Davalli et al. 1995, 1996) and led to a loss of B cells. Reparative processes supported the development of fibrous tissue, while hypoxia induced the production of endothelial growth factors (Vasir et al. 1998) and vascular proliferation by angiogenesis (Zhang et al. 2004; Lai et al. 2005). Connective tissue tended to surround the graft allowing a stable contact with the host vessels, from which capillaries penetrated inside the endocrine tissue. Finally, after 2–3 weeks, there was no longer any morphological evidence of vascular proliferation and remodelling of the tissue, and the engraftment could be considered to be stable.

Modifications of the islets after isolation and purification from the pancreas have been demonstrated (El-Naggar et al. 1993; Morini et al. 2001, 2006), mainly characterized by fragmentation of some islets and a prevalent loss of the most peripheral cells (A and D cells), as revealed by numerical analysis. The present observations have demonstrated that pancreatic islets undergo substantial changes in the remodelling process immediately post-transplant. In fact, partial necrosis led to loss of islet mass, represented in particular by the destruction of the inner B cells (Davalli et al. 1995), and

a consequent significant variation in the percentage of the different cells types in the first few days has been demonstrated. Apoptosis might account for a further loss of cells (Davalli et al. 1996; Barshes et al. 2005).

These early phenomena were followed by a reaggregation and remodelling of the endocrine tissue. After a few days post-transplant, new vessels penetrated the graft from outside, and blood began to flow into the newly formed microvascular network. Vessels clearly penetrated inside the graft from all directions (Kin et al. 2004). Our observations showed vessels connected with both the capsular and the cortical circulation running along the outer endocrine cells. The revascularization process gave rise to a newly formed cordonal-like structure which completed the reorganization of the surviving endocrine tissue inside the islets.

Vajkoczy et al. (1995) described the first signs of angiogenesis about 4 days after the transplant into special skinfold chambers, and completed revascularization at day 10, without further changes on day 14. However, we found that angiogenesis, although becoming rarer, is still present at day 14 post-transplant under the kidney capsule; this observation agrees with data on vascular rearrangement reported for a long time after the transplant of fetal porcine islet-like clusters (Korsgren et al. 1999). However, unlike Lukinius et al. (1995), we never found microvessels lacking an endothelial cell lining, and from our observations, revascularization is always supported by endothelial cells penetrating inside the transplanted islet from outside. This was clearly demonstrated with immunostaining and electron microscopy. Interestingly, endothelial cells already show fenestrations at the interface with endocrine cells at day 7. This feature, characteristic of pancreatic endocrine capillaries, permits a very rapid trans-endothelial diffusion, and supports the precocious functionality of the graft.

From our observations, some differences were evident by comparing graft with native islets. We have studied A, B and D cells because they are known as metabolic controllers of glycaemia, they represent the large majority of the cells in pancreatic islets, and they show a defined location in pancreatic islets *in situ*. Numerical analysis demonstrated that the percentage number of the different cells types in the transplant was different from that of *in situ* islets. Although these data did not change significantly after day 4, in transplanted islets the percentage number of A and D cells was always significantly less than in native islets, while the percentage

number of B cells was always significantly higher. The change in cell percentage could not be correlated with any proliferative mechanism. As shown with the BrdU incorporation data, cell proliferation could not be detected in the post-transplant period. Furthermore, in contrast to the observations on *in situ* islets, A and D cells formed in the graft a largely incomplete crown around the B-cell cores, and they were also frequently found inside the endocrine tissue. Finally, the process of graft revascularization indicates a final vascular arrangement that is rather different from that of native islets.

Thus, following the engraftment, the resulting endocrine tissue was quantitatively and qualitatively different from the initial situation. As a consequence, some conditions related to the cellular composition and to the new microvascular organization affected the efficiency of hormone release. In fact, interactions among cells are known to be critical for a better regulation of the secretory function (Halban et al. 1982; Pipeleers et al. 1982; Hopcroft et al. 1985; Weir & Bonner-Weir, 1990). Direct cell–cell communication occurs through gap junctions (Meda et al. 1983; Orci, 1982; Meda, 1996) and plays an important role in the regulation of cell secretion (Halban et al. 1982; Hopcroft et al. 1985; Weir et al. 1990) such that quantitative changes in the percentage of the cellular population might lead to alterations in the normal secretory function of B cells (Trimble et al. 1982).

Moreover, the importance of the microvascular organization, which permitted sequential perfusion of the different cell types, has been recognized in the functional regulation of *in situ* pancreatic islets (Samols et al. 1988; Menger et al. 1994). This condition supports both a paracrine action (Jörns et al. 1988; Schatz & Kullek, 1980) and an endocrine action through blood flow inside pancreatic islets (Kawai et al. 1995) mediated by the insular hormones.

The specific location of the different types of cells within the islet has suggested that the pattern of blood flow through the islet should have a major role in relation to the intercommunication between cells (Samols et al. 1988; Weir et al. 1990; Liu et al. 1993; Menger et al. 1994). Therefore, the integrity of the microcirculatory network and the orientation of blood flow were considered critical for a better regulation of the secretory function (Menger et al. 1994; Stagner & Samols, 1994).

While the revascularization process was supported by the primary necessity of supplying nutrients and

oxygen, and was demonstrated to be independent of a particular endocrine-cell composition (Beger et al. 1998), it could presumably only partially reflect the pattern of normal blood flow and sequential perfusion through the islet. Although this concept required support from experimental evidence, an alteration of the normal cell–cell communications through blood flow, with an effect on the most precise secretory regulation, should be expected in transplanted islets (Stagner & Samols, 1994; Shi & Täljedal, 1996). Functional studies seem to confirm this reasoning. In fact, modifications of the dynamics of insulin secretion in both cultured (Pai et al. 1993) and transplanted islets (Ricordi et al. 1992; Shi & Täljedal, 1996) have been frequently reported, even in the presence of adequate B-cell mass.

On the basis of our observations on the neovascularization of engrafted islets, we can speculate that there is some relationship with the functional data collected in our model. A total of 600 IEq were transplanted in these animals and this is accepted as the critical mass able to reverse diabetes in a mouse model. Although the reversal of diabetes was achieved around the same time in all animals, without revealing any difference in increased functionality in the immediate post-transplant period, the glucose challenge test demonstrated an improved metabolic control over time post-transplant. Although other phenomena, such as naturally occurring B-cell proliferation (Dor et al. 2004), are responsible for the improved metabolic control under challenge, improved vascularization could be considered a key condition. This seems to be supported by the evidence that functionality appeared improved up to 14 days post-engraftment, when vascularization is still active, and then stabilized and maintained a reasonable glycaemic control over time.

In conclusion, our observations have demonstrated that transplanted islets undergo deep remodelling of their structure due to an interaction with the host and the development of a new microvascular network within the endocrine tissue. After several days, the grafts were revascularized and the capillaries had the characteristic features that facilitate the diffusion of the endocrine secretion. However, the engrafted endocrine tissue was substantially different from *in situ* islets, and the structural changes could represent a basis for the altered regulation of the secretory function reported in the literature, through imperfect intercellular interactions.

Acknowledgement

This work was partially supported by the Italian Consiglio Nazionale delle Ricerche (CNR).

References

- Barshes NR, Wyllie S, Gross JA (2005) Inflammation-mediated dysfunction and apoptosis in pancreatic islet transplantation: implications for intrahepatic grafts. *J Leukoc Biol* **77**, 587–597.
- Beger C, Cirulli V, Vajkoczy P, Halban PA, Menger MD (1998) Vascularization of purified pancreatic islet-like cell aggregates (pseudoislet) after syngeneic transplantation. *Diabetes* **47**, 559–565.
- Bretzel RG, Hering BJ, Schultz AO, Geier C, Federlin F (1996) International islet transplant registry report. In *Yearbook of Cell and Tissue Transplantation* (eds Lanza RP, Chick WL), pp. 153–160. Dordrecht, the Netherlands: Kluwer Academic Publishers.
- Davalli AM, Ogawa Y, Ricordi C, Scharp DW, Bonner-Weir S, Weir GC (1995) A selective decrease in the beta cell mass of human islets transplanted into diabetic nude mice. *Transplantation* **59**, 817–820.
- Davalli AM, Scaglia L, Zangen DH, Hollister J, Bonner-Weir S, Weir GC (1996) Vulnerability of islet in the immediate post-transplantation period: dynamic changes in structure and function. *Diabetes* **45**, 1161–1167.
- Dionne KE, Colton CK, Yarmush ML (1993) Effect of hypoxia on insulin secretion by isolated rat and canine islets of Langerhans. *Diabetes* **42**, 12–21.
- Dor Y, Brown J, Martinez OI, Melton DA (2004) Adult pancreatic beta-cells are formed by self-duplication rather than stem-cell differentiation. *Nature* **429**, 41–46.
- El-Naggar M, Elayat A, Ardawi M, Tahir M (1993) Isolated pancreatic islets of the rat: an immunohistochemical and morphometric study. *Anat Rec* **237**, 489–497.
- Halban PA, Wollheim CB, Blondel B, Meda P, Nieson EN, Mintz DH (1982) The possible importance of contact between pancreatic islet cells for the control of insulin release. *Endocrinology* **111**, 86–94.
- Hering B, Ricordi C (1999) Islet transplantation for patients with type I diabetes. *Graft* **2**, 12–27.
- Heuser M, Wolf B, Vollmar B, Menger MD (2000) Exocrine contamination of isolated islets of Langerhans deteriorates the process of revascularization after free transplantation. *Transplantation* **69**, 756–761.
- Hopcroft DW, Mason DR, Scott RS (1985) Structure–function relationships in pancreatic islets: support for intraislet modulation of insulin secretion. *Endocrinology* **117**, 2073–2080.
- Jörns A, Barklage E, Grube D (1988) Heterogeneities of the islets in the rabbit pancreas and the problem of ‘paracrine’ regulation of islet cells. *Anat Embryol* **178**, 297–307.
- Kawai K, Yokota C, Ohashi S, Watanabe Y, Yamashita K (1995) Evidence that glucagon stimulates insulin secretion through its own receptor in rats. *Diabetologia* **38**, 274–276.
- Kin T, Rajotte RV, Korbitt GS (2004) Reassessment of the vascularization of renal subcapsular islets grafts. *Pancreas* **29**, 59–63.
- Korbitt GS, Warlock GL, Rajotte RV (1997) Islet transplantation. *Adv Exp Med Biol* **426**, 397–410.
- Korsgren O, Christofferson R, Jansson L (1999) Angiogenesis and angioarchitecture of transplanted fetal porcine islet-like cell clusters. *Transplantation* **68**, 1761–1766.
- Lai Y, Schneider D, Kiszun A, et al. (2005) Vascular endothelial growth factor increases functional beta-cell mass by improvement of angiogenesis of isolated human and murine pancreatic islets. *Transplantation* **79**, 1530–1536.
- Liu Y, Guth PH, Kaneko K, Livingston EH, Brunicaardi FC (1993) Dynamic in vivo observation of rat islet microcirculation. *Pancreas* **8**, 15–21.
- Lukinius A, Jansson L, Korsgren O (1995) Ultrastructural evidence for blood microvessels devoid of an endothelial cell lining in transplanted pancreatic islets. *Am J Pathol* **146**, 429–435.
- Mattsson G, Danielsson A, Kriz V, Carlsson PO, Jansson L (2006) Endothelial cells in endogenous and transplanted pancreatic islets: differences in the expression of angiogenic peptides and receptors. *Pancreatol* **6**, 86–95.
- Meda P, Michaels RL, Halban PA, Orci L, Sheridan JD (1983) In vivo modulation of gap junctions and dye coupling between b-cells of the intact pancreatic islet. *Diabetes* **32**, 858–868.
- Meda P (1996) The role of gap junction membrane channels in secretion and hormonal action. *J Bioenerg Biomembr* **28**, 369–377.
- Menger MD, Jaeger S, Walter P, Feifel G, Hammersen F, Messmer K (1989) Angiogenesis and hemodynamics of microvasculature of transplanted islets of Langerhans. *Diabetes* **38** (Suppl. 1), 199–201.
- Menger MD, Vajkoczy P, Beger C, Messmer K (1994) Orientation of microvascular blood flow in pancreatic islet isografts. *J Clin Invest* **93**, 2280–2285.
- Menger MD, Yamauchi J, Vollmar B (2001) Revascularization and microcirculation of freely grafted islets of Langerhans. *World J Surg* **25**, 509–515.
- Morini S, Braun M, Cicalese L, Gaudio E, Benedetti E, Rastellini C (2001) Isolated pancreatic islets: structural and ultrastructural analysis. *Transplantation Proc* **33**, 668–669.
- Morini S, Braun M, Onori P, et al. (2006) Morphological changes of isolated rat pancreatic islets: a structural, ultrastructural and morphometric study. *J Anat* **209**, 381–392.
- Orci L (1982) Macro- and micro-domains in the endocrine pancreas. *Diabetes* **31**, 538–565.
- Pai GM, Slavin BG, Tung P, et al. (1993) Morphologic basis for loss of regulated insulin secretion by isolated rat pancreatic islets. *Anat Rec* **237**, 498–505.
- Pieper GM, Jordan M, Adams MB, Roza AM (1995) Syngeneic pancreatic islet transplantation reverses endothelial dysfunction in experimental diabetes. *Diabetes* **44**, 1106–1113.
- Pipeleers D, in’t Veld P, Maes E, Van De Winkel M (1982) Glucose-induced insulin release depends on functional cooperation between islet cells. *Proc Natl Acad Sci USA* **79**, 7322–7325.
- Rastellini C, Shapiro R, Corry R, Fung JJ, Starzl TE, Rao AS (1997) Treatment of isolated pancreatic islets to reverse pancreatectomy-induced and insulin dependent type I diabetes in humans: a 6 year experience. *Transplantation Proc* **29**, 746–747.

- Ricordi C, Tzakis AG, Carroll PB, et al.** (1992) Human islet isolation and allotransplantation in 22 consecutive cases. *Transplantation* **53**, 407–414.
- Ricordi C, Strom TB** (2004) Clinical islet transplantation: advances and immunological challenger. *Nat Rev Immunol* **4**, 259–268.
- Robertson RP** (2004) Islet transplantation as a treatment for diabetes – A work in progress. *N Engl J Med* **350**, 694–705.
- Ryan EA, Paty BW, Senior PA, et al.** (2005) five-year follow-up after clinical islet transplantation. *Diabetes* **54**, 2060–2069.
- Samols E, Stagner JI, Ewart RBL, Marks V** (1988) The order of islet microvascular cellular perfusion is B → A → D in the perfused rat pancreas. *J Clin Invest* **82**, 350–353.
- Schatz H, Kullek U** (1980) Studies on the local (paracrine) actions of glucagon, somatostatin and insulin in isolated islets of rat pancreas. *FEBS Lett* **122**, 207–210.
- Shapiro AM, Lakey JR, Ryan EA, et al.** (2000) Islet transplantation in seven patients with type I diabetes mellitus using a glucocorticoid-free immunosuppressive regimen. *N Eng J Med* **343**, 230–238.
- Shapiro JAM, Ricordi C, Hering BJ, et al.** (2006) International trial of the Edmonton protocol for islet transplantation. *N Engl J Med* **355**, 1318–1330.
- Shi CL, Täljedal IB** (1996) Dynamics of glucose-induced insulin release from mouse islets transplanted under the kidney capsule. *Transplantation* **62**, 1312–1318.
- Stagner JI, Samols E** (1994) Altered microcirculation and secretion in transplanted islet. *Transplantation Proc* **26**, 1100–1102.
- Trimble ER, Halban PA, Wollheim CB, Renold AE** (1982) Functional differences between rat islets of ventral and dorsal pancreatic origin. *J Clin Invest* **69**, 405–413.
- Tzakis AG, Ricordi C, Alejandro R, et al.** (1990) Pancreatic islet transplantation after upper abdominal exenteration and liver replacement. *Lancet* **336**, 402–405.
- Vajkoczy P, Menger MD, Simpson E, Messmer K** (1995) Angiogenesis and vascularization of murine pancreatic islet graft. *Transplantation* **60**, 123–127.
- Vasir B, Aiello LP, Yoon KH, Quickel RR, Bonner-Weir S, Weir GC** (1998) Hypoxia induces vascular endothelial growth factor gene and protein expression in cultured rat islet cells. *Diabetes* **47**, 1894–1903.
- Wang RN, Paraskevas S, Rosemberg L** (1999) Characterization of integrin expression in islets isolated from hamster, canine, porcine, and human pancreas. *J Histochem Cytochem* **47**, 499–506.
- Weir GC, Bonner-Weir S** (1990) Islets of Langerhans: the puzzle of intraislet interactions and their relevance to diabetes. *J Clin Invest* **85**, 983–987.
- Zhang N, Richter A, Suriawinata J, et al.** (2004) Elevated vascular endothelial growth factor production in islets improves islet graft vascularization. *Diabetes* **53**, 963–970.